

9927 8698 NI YCAN  
NACA TN 3633 7666

TECH LIBRARY KAFB, NM  
0066422

# NATIONAL ADVISORY COMMITTEE FOR AERONAUTICS

TECHNICAL NOTE 3633

ANALYSIS OF THE ULTIMATE STRENGTH AND OPTIMUM PROPORTIONS  
OF MULTIWEB WING STRUCTURES

By B. Walter Rosen

Langley Aeronautical Laboratory  
Langley Field, Va.



Washington  
March 1956

TECHNICAL NOTE

3633



## NATIONAL ADVISORY COMMITTEE FOR AERONAUTICS

## TECHNICAL NOTE 3633

ANALYSIS OF THE ULTIMATE STRENGTH AND OPTIMUM PROPORTIONS  
OF MULTIWEB WING STRUCTURES

By B. Walter Rosen

## SUMMARY

A structural-efficiency analysis of multiweb wing structures is presented. Minimum structural weight is shown as a function of the design variables (bending moment, wing chord, depth, and skin thickness) in a manner which makes comparisons possible with structures of different materials or with other types of construction.

The structural-efficiency chart presented is based on equations developed to relate ultimate bending strength of multiweb beams which fail in the local buckling mode to beam proportions and material properties. The equations are substantiated by the presented results of bending tests of multiweb beams with both fabricated and integral web-skin attachments.

## INTRODUCTION

The wings of supersonic airplanes must satisfy severe strength and stiffness requirements and yet be relatively thin and of minimum weight. In order to measure the relative structural efficiency of various types of thin-wing construction, the present paper considers, as a standard for comparison, the minimum-weight design of thick-skin multiweb wing structures.

The maximum strength and structural efficiency of multiweb structures has been studied previously by other investigators (for example, refs. 1, 2, and 3); however, this investigation utilizes a somewhat different strength analysis and includes the effect of skin-thickness requirements on structural efficiency.

The results are presented in the form of a structural-efficiency chart where minimum structural weight is plotted as a function of the structural index for constant values of the ratio of wing depth to skin thickness. The structural index incorporates the following basic design specifications: bending moment, structural chord, and wing depth. For the range of these variables considered, web thickness and spacing have

been made optimum to yield minimum weight for 7075-T6 (formerly 75S-T6) aluminum-alloy multiweb beams, but skin thickness has been retained as a parameter because a minimum or maximum skin gage is frequently specified to satisfy stiffness or other design requirements.

The efficiency study is based on an empirical relationship between maximum bending strength and structural proportions for beams so designed that the wrinkling mode is eliminated (see refs. 4 and 5) and instability occurs at the higher stresses associated with the local mode. The equations used are supported by the results of bending tests of integral and fabricated beams.

The material presented in this paper was originally included in a thesis submitted to the Virginia Polytechnic Institute in partial fulfillment of the requirements for the master of science degree in Applied Mechanics on May 3, 1955.

#### SYMBOLS

$A_i$	average cross-sectional area per chordwise inch, in.
$A_i/h$	solidity
$b$	width of plate element, in.
$C = \frac{3.5}{k_W} \frac{\sigma_2}{E} (\epsilon_2)^{1/2}$	
$c$	structural chord or overall width of multiweb beam, in.
$E$	Young's modulus, ksi
$E_{sec}$	secant modulus, ksi
$E_{sec_2}$	$\sigma_2/\epsilon_2$ , ksi
$E_{tan}$	tangent modulus, ksi
$E_2$	strength modulus, $\sigma_2/\sqrt{\epsilon_2}$ , ksi
$h$	wing depth, in.

k	nondimensional buckling-stress coefficient
M	bending moment, in-kips
M <sub>F</sub>	bending moment per cell at failure, in-kips
M <sub>1</sub>	bending moment per chordwise inch at failure, in-kips/in.
M' <sub>1</sub>	average bending moment per chordwise inch at failure resisted by webs, in-kips/in.
M <sub>1</sub> /h <sup>2</sup>	structural index, ksi
n	number of webs
P	compressive load, kips
t	plate thickness, in.
w	weight density, lb/in. <sup>3</sup>
α	web stress-distribution coefficient
$\beta = \frac{b_W/t_W}{b_S/t_S}$	
ε	strain
ε <sub>2</sub>	strain at which $E_{\tan} = \frac{1}{2}E_{\sec}$
η	nondimensional plasticity correction factor; $\eta = 1$ for $\sigma_S \leq \sigma_2$ $\eta = \left(\frac{E_{\sec}}{E_{\sec 2}}\right)^{1/2}$ for $\sigma_S \geq \sigma_2$
σ	stress, ksi
σ <sub>S</sub>	average plate stress at failure, calculated, ksi
σ <sub>2</sub>	stress at which $E_{\tan} = \frac{1}{2}E_{\sec}$ , ksi

## Subscripts:

a	web-skin attachment member
c	crushing
cr	critical
e	edge
min	minimum
S	compression skin
T	tension skin
W	web

## ULTIMATE STRENGTH OF MULTIWEB STRUCTURES

The ultimate strength and the mode of failure of multiweb structures depend upon the stiffness of the webs and of the attachment of the webs to the compression skin. When the web-skin attachment has a low deflectional stiffness, instability will occur in the wrinkling mode. When the attachment is of sufficient stiffness, the behavior of the beam will approach that of an integral multiweb beam and instability will occur in the local buckling mode. Because the changes in attachment design which are required to avoid wrinkling instability involve little or no weight increase, structures designed to buckle in the local mode are more efficient and, hence, are treated in this paper.

The ultimate strength of multiweb beams which buckle in the local mode is calculated by considering the load in each of the plate elements at the failing moment. The moment resisted per cell is

$$M_F = M_S + M_W \quad (1)$$

The crippling strength of each bay of the compression skin can be related to the width and thickness of the plate. The associated bending moment, when the tension skin is of adequate design, is

$$M_S = \sigma_S b_S t_S b_W \quad (2)$$

The moment resisted by each web can be determined from the in-plane web bending-stress distribution existing when the compression-skin load is a maximum. Thus,

$$M_W = \alpha \sigma_e b_W^2 t_W \quad (3)$$

where  $\alpha$  depends upon the depthwise stress distribution and  $\sigma_e$  is the stress at the junction of the web and the compression cover skin.

The relationships between the strength and the proportions of the various multiweb plate elements are developed in the following sections from consideration of the available experimental data.

#### Cover-Skin Strength

References 6 and 7 have shown that the relationship between plate ultimate strength, dimensions, and material properties which has been developed for compression tests of plates in V-groove edge fixtures is also useful for determining the ultimate strength of plate elements of longitudinally stiffened compression panels which buckle in the local mode. It is assumed herein that the same equation is applicable to the cover skin of a multiweb beam.

The crippling strength of plates in V-groove edge fixtures is given empirically in reference 7 as

$$\sigma_S = 1.75 E_2 \frac{t_S}{b_S} \quad (\sigma_S \leq \sigma_2) \quad (4)$$

where  $E_2$  is called a crippling-strength modulus for edge-supported plates and is defined by

$$E_2 = \frac{\sigma_2}{(\epsilon_2)^{1/2}}$$

where  $\sigma_2$  and  $\epsilon_2$  are the coordinates of the point on a compressive stress-strain curve at which the tangent modulus is equal to one-half the secant modulus for a material.

Equation (4) is valid only for stresses below  $\sigma_2$ , but it can be extended to higher stress ranges as follows:

$$\sigma_S = 1.75 \eta E_2 \frac{t_S}{b_S}$$

Because stresses higher than  $\sigma_2$  are rarely encountered in practical wing structures, the application that follows will be limited to the thick-skin proportions to which equation (4) is applicable.

Substituting equation (4) into equation (2) gives

$$M_S = 1.75 E_2 b_W t_S^2 \quad (5)$$

#### Web Strength

The webs are edge-supported plates subjected to a bending-stress distribution, and each web resists a bending moment given by equation (3). The edge stress  $\sigma_e$  has a maximum value equal to the maximum edge stress of the cover plates. In the development of equation (4) (see ref. 7), a maximum edge stress equal to  $\sigma_2$  was assumed. The moment in the webs at ultimate load is assumed herein to approach that resulting from a rectangular bending-stress distribution of magnitude  $\sigma_2$ ; that is,

$$M_W = \frac{1}{4} \sigma_2 b_W^2 t_W \quad (6)$$

#### Beam Strength

By substituting equations (5) and (6) into equation (1), the maximum moment resisted by each cell of a multiweb beam is

$$M_f = 1.75 E_2 b_W t_S^2 + \frac{1}{4} \sigma_2 b_W^2 t_W \quad (7)$$

The validity of equation (7) is demonstrated by application to test results of both integral and fabricated beams tested in pure bending. The equation is valid only when the webs and the attachments are of sufficient stiffness to support the cover until it reaches the stress given by equation (4). (See appendix.)

## EXPERIMENTAL DATA

Bending tests of integral and fabricated multiweb beams were performed in the combined load testing machine of the Langley structures research laboratory in order to determine the maximum strength of multiweb beams with stiff web-skin attachments. The results of the integral-beam tests are used to substantiate the assumptions made concerning web behavior, as regards both stress distribution and minimum thickness requirements, and skin strength. The results of the fabricated-beam tests are used to determine the applicability of the maximum-strength equations to practical, riveted multiweb structures.

## Test Specimens

The integral beams consisted of one or two cells. (See fig. 1.) The one-cell integral beams were drawn, square tubes with thickness ratio  $t_w/t_s$ , and skin thickness  $t_s$  varied by machining skin and/or webs to the desired thicknesses. The two-cell integral beams were constructed from E-section extrusions by riveting a tension cover to the web flanges and machining the webs and compression skins to obtain the various values of  $t_w/t_s$ . The three-cell fabricated beams were constructed by using two extruded angles riveted together to form a channel-type web. (See fig. 1.) The cross-sectional dimensions of the angle extrusions are shown in figure 1. Material properties of all test specimens are presented in table I; specimen dimensions and the significant dimension ratios are given in tables II and III, respectively.

## Test Results

Integral beams.- The results of the tests of one- and two-cell integral beams (see table IV(a)) were used to determine the validity of the assumption that  $\alpha$  in equation (3) equals  $1/4$ .

The value of  $\alpha$  can be determined from equation (3), when  $\sigma_e = \sigma_2$ , as

$$\alpha = \frac{1}{\sigma_2} \frac{M_w}{b_w^2 t_w}$$

or, where  $M'_1 = \frac{M_W}{b_S}$ ,

$$\alpha = \frac{1}{\sigma_2} \frac{M'_1}{b_W^2} \frac{b_S}{t_W} \quad (8)$$

The web moment can be determined by subtracting the computed skin moment (see eq. (5)) from the experimental failing moment.

Figure 2 is a plot of  $M'_1/\sigma_2 b_W^2$  against  $t_W/b_S$  for the integral beams. The results for those beams that do not satisfy the web-thickness requirements of

$$\left(\frac{t_W}{t_S}\right)_{\min} = C^{1/3} \left(\frac{b_W}{t_S}\right)^{1/3} \quad (9a)$$

and

$$\left(\frac{t_W}{t_S}\right)_{\min} = \frac{1}{3} \frac{b_W}{t_S} \frac{t_S}{b_S} \quad (9b)$$

are omitted. (These equations are developed as eqs. (A5) and (A9) in the appendix.) The test points, in general, approach the line representing equation (3) and plotted for  $\alpha = 1/4$ .

Fabricated beams.- In order to compare the experimental results for the fabricated beams with the calculated strength values, equation (7) must be modified to include the effect of the web attachment flanges. The moment carried by compact attachment members is approximated by

$$M_a = \sigma_2 A_a (b_W - t_S - t_a) \quad (10)$$

where  $t_a$  equals twice the distance from the inner surface of the compression skin to the centroid of the attachment member (for a channel, this is the flange thickness) and  $A_a$  is the area of the web-skin attachment member.

Hence, the moment carried per cell by fabricated multiweb beams with webs of sufficient thickness to satisfy equations (9) is

$$M_F = M_S + M_W + M_a \quad (11)$$

Table IV(b) gives a comparison of the experimental failing moments and the total computed failing moments for the three-cell fabricated beams.

Figure 3 is a plot of the calculated failing moment against the experimental failing moment. The 45° line represents perfect agreement. Each group of points corresponds to a group of beams of constant skin thickness in which  $b_g/t_g$  was varied from 20 to 40. Beams with webs of insufficient thickness to satisfy equations (9) are plotted as square test points. For these beams the predicted failing moment is the bending moment at which the beam would crush and is based on the equations presented in the appendix in the section entitled "Web Crushing". The calculated moment for all other beams is the value computed from equation (11) modified to allow for three cells, four webs, and overhanging skin. (See table IV(b).)

The agreement of calculated and experimental results indicates that the assumptions for cover strength and web stress distribution at the maximum moment result in a valid approximation of the bending strength of multiweb beams. The assumption that the cover-skin strength of one bay of a fabricated multiweb beam is equal to that of a similar plate in a V-groove edge-fixture compression test appears valid for the beams tested. This assumption may be somewhat conservative when the torsional stiffness of the web attachment is increased (as in the case of beams with heavy T-cap attachment members) and unconservative when the attachment stiffness is decreased (as in the case of beams fabricated with formed-channel webs). (See, for example, ref. 8.)

#### STRUCTURAL EFFICIENCY OF MULTIWEB CONSTRUCTION

The equations relating maximum bending strength to beam proportions can be presented in the form of a structural-efficiency chart, where minimum structural weight is plotted as a function of the design variables.

The design conditions for a multiweb wing (bending moment per chordwise inch  $M_1$ , wing depth  $h$ , and a minimum skin gage  $t_g$ ) are incorporated into the parameters used in this efficiency study. These parameters are (1) the structural index  $M_1/h^2$ , which is a measure of the loading intensity and a function of material properties and nondimensional quantities, and (2) the ratio of depth to skin thickness  $h/t_g$ , a nondimensional measure of the skin gage needed to satisfy stiffness or other requirements. Structural weight, the factor which is to be minimized, is directly proportional to the cross-sectional solidity  $A_1/h$ . Only the cross-sectional area of the compression skin and the supporting webs is considered, as the amount of tension material required is essentially independent of web size and spacing.

For each  $h/t_g$  value, web size and spacing have been varied to obtain a curve of minimum weight plotted against loading intensity which represents

optimum web proportions. In order to maximize the moment of inertia of the beam cross section, material should be located as far from the neutral axis as possible. Therefore, webs for optimum design are generally of the minimum thickness necessary to satisfy the support requirements specified by equations (9).

In order to determine the efficiency curves, the solidity and structural index can be expressed as functions of the beam dimensions as follows:

$$A_1 = \frac{1}{b_S} (b_S t_S + b_W t_W) \quad (12)$$

which can be expressed nondimensionally as

$$\frac{A_1}{h} = \frac{t_S}{h} + \frac{t_W}{t_S} \frac{t_S}{h} \frac{h}{b_S} \frac{b_W}{h} \quad (13)$$

where

$$\frac{b_W}{h} = 1 - \frac{t_S}{h} \quad (14)$$

Also,

$$M_1 = \frac{1}{b_S} M_F \quad (15)$$

When equation (7) is substituted into equation (15) and expressed in dimensions of stress alone, the following equation results:

$$\frac{M_1}{h^2} = 1.75 E_2 \left( \frac{t_S}{h} \right)^2 \frac{h}{b_S} \frac{b_W}{h} + 0.25 \sigma_2 \frac{t_W}{t_S} \frac{t_S}{h} \frac{h}{b_S} \left( \frac{b_W}{h} \right)^2 \quad (16)$$

The dimension ratios used were chosen because  $h/t_S$  will be specified by design data, and  $t_W/t_S$  will be specified by equations (9). The ratio  $b_W/h$  is a function of  $h/t_S$  alone. (See eq. (14).)

The relationship between solidity and structural index given by equations (13) and (16) is plotted in figures 4 and 5 for 7075-T6 aluminum-alloy structures. This was done by assuming values of  $h/t_S$  and  $h/b_S$  and solving for  $t_W/t_S$  from equations (9). The larger of the two values calculated from equations (9) is used in equations (13) and (16) to determine the index and the solidity. With  $h/t_S$  held constant,  $h/b_S$  is

varied to obtain one of the curves in figure 4. Then,  $h/t_S$  is varied for a constant  $h/b_S$  to obtain one of the curves of figure 5.

In order to lend perspective to these diagrams, the weight of a fictitious structure consisting of two unsupported cover skins acting at the stress  $\sigma_2$  has been calculated and is given by the line labeled "Max. eff." For such a structure,

$$\frac{M_1}{h^2} = \frac{1}{h^2} \sigma_2 t_S b_W \approx \sigma_2 \frac{t_S}{h}$$

and

$$\frac{A_1}{h} = \frac{t_S}{h}$$

Solving the two equations simultaneously gives

$$\frac{A_1}{h} = \frac{1}{\sigma_2} \frac{M_1}{h^2} \quad (17)$$

Multiweb beams are heavier than this fictitious structure because

- (1) Cover skins for most proportions have maximum average stresses below  $\sigma_2$  as a result of local instability.
- (2) Web material is needed to support the covers.

## DISCUSSION

### Efficiency Curves

The lower envelope to the curves of figure 4 represents the minimum structural weight required to support the design moment when all interior dimensions may be freely varied. However, if the skin thickness or web spacing is specified, there may be an increase in the minimum weight attainable, and the appropriate curves of figures 4 and 5 should be used.

The envelope to the efficiency curves of figure 4 is shown in figure 5 as the "strength envelope" and is similar to what has been calculated by investigators of the weight-strength problem (refs. 1 and 3). In addition to the differences in minimum structural weight resulting from differences in strength analyses, the efficiency study of the present paper shows the effect on minimum weight of skin-gage requirements.

For given design conditions, each efficiency curve of figure 4 represents one skin thickness, and, at zero load, the intercept of each curve represents the solidity resulting from the skin alone. The increase in weight above this intercept represents the web weight required to stabilize the compression skin. As shown by the relative position of these  $h/t_s$  curves, an increase in skin thickness at a constant value of the structural index generally results in increased weight. For such proportions, the minimum skin thickness that meets stiffness or other requirements will result in the lightest weight structure that can satisfy the design requirements. However, it is of interest to note that, in certain regions (generally, low index values), increasing the skin thickness at a constant index value results in a decrease in weight. In such ranges (for example, the curves for  $h/t_s$  values of 40 and 50, between index values of 1 and 2), increasing the skin thickness above the required minimum at a given index value will result in a lighter structure, and the envelope value of skin thickness will be most efficient for stiffness as well as strength.

The curves of figure 4 can be used

- (1) To determine the minimum-weight structure for given design conditions (that is, overall dimensions, strength, and stiffness)
- (2) To determine the weight penalties associated with the use of nonoptimum proportions
- (3) To compare the weight of this type of construction with any other

These uses are discussed in greater detail in the discussion which follows.

#### Beam Proportions

The optimum structural proportions corresponding to any point on the efficiency curves can be determined by use of the presented curves and equations. For the design values of  $M_1$ ,  $h$ , and  $t_s$ , the solidity can be found from figure 4 and the  $h/b_s$  ratio can be found from figure 5. Equation (13) can be used to determine  $t_w/t_s$ . The web size and spacing are then readily evaluated.

Several alternate methods involving more labor and resulting, perhaps, in greater accuracy may be employed to find web size and spacing if it is so desired. These include the following:

- (1) Determine the solidity from figure 4. Solve equations (13) and (16) simultaneously to determine  $t_w/t_s$  and  $t_s/b_s$ .

(2) Determine the solidity from figure 4. Find  $t_W/b_S$  from equation (13); thus,

$$\frac{t_W}{b_S} = \left( \frac{A_1}{h} - \frac{t_S}{h} \right) \frac{h}{b_W}$$

Find  $b_S/t_S$  from equation (9a); thus,

$$\frac{b_S}{t_S} = C^{1/3} \left( \frac{b_W}{t_S} \right)^{1/2} \frac{b_S}{t_W}$$

or, from equation (9b),

$$\frac{b_S}{t_S} = \left( \frac{1}{3} \frac{b_W}{t_S} \frac{b_S}{t_W} \right)^{1/2}$$

The larger  $b_S/t_S$  value must be used to determine web spacing.

#### Buckling Below Limit Load

Many structures must satisfy not only strength and stiffness criteria but also a requirement that there be no skin buckling below design limit load; that is,  $\frac{2}{3} M_F$ . For each  $h/t_S$  value, there is one point on the optimum curve which defines a structure that will buckle at limit load. Structures designed for higher index values will buckle above limit load and structures designed for lower index values will buckle below limit load. In order to determine the critical value of  $b_S/t_S$  for any  $h/t_S$  value, let

$$M_{cr} = \frac{2}{3} M_F \quad (18)$$

For the 7075-T6 aluminum alloy, buckling will be elastic and the stress distribution will be triangular. Hence, in equation (3),

$$\alpha = \frac{1}{6}$$

and

$$M_{i_{cr}} = \sigma_{cr} t_S b_W + \frac{1}{6} \sigma_{cr} b_W^2 t_W \frac{1}{b_S}$$

where

$$\sigma_{cr} = k_S E \left( t_S / b_S \right)^2$$

Hence,

$$\frac{M_{1cr}}{h^2} = k_S E \left( \frac{t_S}{b_S} \right)^2 \left[ \frac{t_S}{h} \frac{b_W}{h} + \frac{1}{6} \frac{t_W}{t_S} \frac{t_S}{b_S} \left( \frac{b_W}{h} \right)^2 \right] \quad (19)$$

Substituting equations (9a), (9b), (15), (16), and (19) into equation (18) yields

$$\left( \frac{t_S}{b_S} \right)^2 + \frac{t_S}{b_S} \left[ \frac{6}{c^{1/3}} \left( \frac{t_S}{h} \right)^{4/3} \left( \frac{h}{b_W} \right)^{4/3} \right] - \left[ \frac{7E_2}{c^{1/3} k_S E} \left( \frac{t_S}{h} \right)^{4/3} \left( \frac{h}{b_W} \right)^{4/3} + \frac{\sigma_2}{k_S E} \right] = 0 \quad (20)$$

and

$$\left( \frac{t_S}{b_S} \right)^3 + \frac{t_S}{b_S} \left[ 18 \left( \frac{t_S}{h} \right)^2 \left( \frac{h}{b_W} \right)^2 - \frac{\sigma_2}{k_S E} \right] - \left[ 21 \frac{E_2}{k_S E} \left( \frac{t_S}{h} \right)^2 \left( \frac{h}{b_W} \right)^2 \right] = 0 \quad (21)$$

Equation (20) contains the web criterion of equation (9a), and equation (21) contains that of equation (9b). The higher value of  $t_S/b_S$  given by these two equations for any value of  $h/t_S$  is the appropriate one.

The computed values of  $t_S/b_S$  are indicated by the tick marks on the curves of figure 4. Proportions to the left of these values on any curves must be modified to eliminate buckling below limit load. This modification results in a small weight change for shallow beams and a large change for deep or thin-skin beams.

#### Shear Loads

This analysis considers bending moments as the only loads on the structure. In actual aircraft the problem of carrying vertical shear

in the webs must be considered. For deep wings, the webs called for by this analysis offer a large area to resist shear loads. For the shallow wings with low  $h/t_S$  values, however, additional shear area may be required.

#### Effect of Differences Between Actual and Ideal Structures

Attachment members.- Equations (5) and (6) express the maximum moment carried by the skin and flat-sheet portion of the web of a fabricated beam if the web-skin connection is a strongly riveted one. This requires small rivet-offset distances. (See ref. 5.) An attachment member, either the flange of a channel web or an angle cap or T-cap, must usually be considered. Such an attachment member adds to the solidity of a beam but it also adds to the moment-carrying capacity. The stress carried by small attachment members will be approximately equal to the edge stress  $\sigma_2$ .

By a development similar to that of equation (17), it can easily be shown that, when attachment members are added to an optimum design which is selected from figure 4, the deviation of the actual beam from the optimum integral beam (when both are plotted in fig. 4) is approximately along a line of the same slope as the maximum-efficiency curve.

On the basis of this development, the range over which attachment members increase beam efficiency can be determined. When the slope of any  $h/t_S$  curve equals  $1/\sigma_2$ , the slope of the maximum-efficiency curve, it becomes more efficient to move to the right in figure 4 by adding T-caps or angle caps than to decrease web spacing and increase web thickness.

Neutral-axis location.- When because of cover-skin buckling, unequal thickness of cover skins, or other lack of beam symmetry, the neutral-axis location is not at the web midheight, the maximum-strength equations are affected. The change in neutral-axis location results in unequal edge stresses at the two covers and a resultant axial force as well as a bending moment acting on the webs. In general, the effect of this change on the maximum-strength equation (eq. (7)) will be small. For example, consider a web stress distribution with the distance of the neutral axis from each cover changed by 20 percent, that is, 40 percent of the web under tensile stress. If the stresses are again approximated by a rectangular stress distribution of magnitude  $\sigma_e$ , the plate will have an axial compression force equal to  $0.2\sigma_e b_W t_W$  and a moment equal to  $0.24\sigma_e b_W^2 t_W$ . The moment is essentially that given in equation (6), and it is seen that the effect is a small one. For beams with an adequate tension cover, the effect of a neutral-axis shift on equation (5) will also be negligible.

### Use of Other Materials

Structures of materials other than the 7075-T6 aluminum alloy considered can be compared with the structures represented in figure 4. For the structure in question, the value of the structural index can be obtained by test or computations, and the weight comparison is made by determining the equivalent solidity and the ratio of depth to skin thickness by utilizing the ratios of densities and shear moduli of the materials.

In order to obtain identical torsional stiffness in the newly selected material and the reference material, let

$$b_{w_x} G_x t_{s_x} = G_r t_{s_r} b_{w_r}$$

where  $G$  is the shear modulus of elasticity, subscript  $r$  refers to reference material, and subscript  $x$  refers to other material.

Except for very thin wings,  $b_{w_r} \approx b_{w_x}$  and the ratio of the equivalent depth to the skin thickness is given by

$$\left(\frac{h}{t_s}\right)_r = \left(\frac{h}{t_s}\right)_x \frac{G_r}{G_x} \quad (22)$$

The equivalent solidity for a direct weight comparison is the computed solidity modified as follows:

$$\left(\frac{A_1}{h}\right)_r = \left(\frac{A_1}{h}\right)_x \frac{w_x}{w_r} \quad (23)$$

### CONCLUDING REMARKS

Equations have been presented which relate the maximum bending strength of multiweb beams which fail in the local buckling mode to the beam proportions and material properties. The experimental results, upon which the equations are based, were also used to establish criteria for the minimum web size required to support the covers satisfactorily.

The expressions for maximum strength have been used in a structural-efficiency analysis which shows minimum weight as a function of the design specifications. For multiweb wing structures, the significant weight

measure is the wing solidity, or the percent of cross section occupied by the compression skin and supporting material; the strength parameter is the structural index, or the ratio of the design moment per chordwise inch to the square of the wing depth; and the skin-thickness requirements are measured by the ratio of wing depth to skin thickness. The efficiency analysis presented enables the determination of the minimum-weight design and the weight required to satisfy both the strength and stiffness requirements. Establishment of the optimum-proportion curves also permits the evaluation of the effects on structural weight of deviations from the optimum, whether such deviations be in the form of changed dimensions, different materials, or other types of construction.

Langley Aeronautical Laboratory,  
National Advisory Committee for Aeronautics,  
Langley Field, Va., December 15, 1955.

## APPENDIX

## WEB REQUIREMENTS

In the derivation of equation (7), it is assumed that the webs and the attachments are of sufficient stiffness to insure cover buckling in the local mode and support the cover until it reaches the stress given by equation (4). In order to prevent failure at lower stresses, web crushing and premature web buckling must be avoided.

## Web Crushing

The webs must not fail under the crushing loads resulting from beam bending. The crushing force per unit length of web is the depthwise component of the loads in the covers, that is,

$$\sigma_c t_W = P \frac{2\epsilon_e}{b_W} \quad (A1)$$

Substituting for the cover load  $P$  gives

$$\sigma_c = \frac{2\sigma_S b_S t_S}{t_W b_W} \epsilon_e \quad (A2)$$

The critical crushing stress is taken as

$$\sigma_{c_{cr}} = k_W E \left( \frac{t_W}{b_W} \right)^2 \quad (A3)$$

The minimum required web thickness to avoid crushing is determined by equating  $\sigma_c$  and  $\sigma_{c_{cr}}$ . This results in the following equation:

$$\left( \frac{t_W}{b_W} \right)^2 \frac{t_W}{t_S} \frac{b_W}{b_S} = \frac{2\sigma_S}{k_W E} \epsilon_e \quad (A4)$$

By substituting the assumed values of  $\sigma_S$  from equation (4) and with  $\epsilon_e = \epsilon_2$ , at ultimate load the following equation is obtained:

$$\left( \frac{t_W}{t_S} \right)_{\min} = c^{1/3} \left( \frac{b_W}{t_S} \right)^{1/3} \quad (A5)$$

where

$$C = \frac{3.5}{k_W} \frac{\sigma_2}{E} (\epsilon_2)^{1/2} \quad (A6)$$

The value of  $k_W$  can be determined from the experimental results for the integral beams. For this purpose, equation (A5) can be modified to account for the effect of the unequal number of webs and cover-skin bays. Thus,

$$\left(\frac{t_W}{t_S}\right)_{\min} = \left[ \left(\frac{n-1}{n}\right) C \left(\frac{b_W}{t_S}\right) \right]^{1/3} \quad (A7)$$

The dimensions of the integral beams were substituted into equation (A7) and values were obtained for  $C$ . The value selected, corresponding to simultaneous crushing and bending failures, was based on the observed beam behavior. The value corresponds to  $k_W = 3$ , which approaches a clamped-edge condition.

#### Web Buckling

In general, the webs will tend either to stabilize or to destabilize the covers, with a resulting change in the buckling-stress coefficient  $k_S$  from the simple support value of 4. Beam proportions considered in the efficiency analysis are restricted to those which result in a value of  $k_S$  which is not significantly lower than 4, so that the supporting structure will not be the source of instability. From reference 2, it is found that, above  $\beta = 3$ ,  $k_S$  decreases rapidly and the minimum  $t_W$  to avoid serious web buckling is herein chosen so that

$$\beta = \frac{b_W/t_W}{b_S/t_S} \leq 3 \quad (A8)$$

Therefore, the minimum thickness ratio is given by

$$\left(\frac{t_W}{t_S}\right)_{\min} = \frac{1}{3} \frac{b_W}{t_S} \frac{t_S}{b_S} \quad (A9)$$

From the experimental results, it can be seen that the web-buckling criterion (eq. (A9)) is conservative. For example, consider the following test results for beam specimens B-4 and V-4 which are identical in

construction. Specimen B-4 was tested in pure bending, and, although the beam had  $\beta = 4$ , the maximum-strength equations of this paper predict the failing moment within 5 percent of the experimental value. Buckling was initiated by web instability at 250 in-kips, or only 56 percent of maximum load.

In order to produce even more severe web buckling, specimen V-4 was tested in bending with an applied shear load equal to the computed critical shear load. The combined loads resulted in buckling when the maximum moment on the test section was only 27 percent of the maximum moment at failure. These buckles also had a negligible effect on ultimate strength.

Equations (A5) and (A9) are plotted in figure 6 for a typical  $h/t_g$  value to show the region in which each criterion governs. The higher value of  $(t_w/t_g)_{\min}$  should be used. When equations (A5) and (A9) are satisfied, equation (7) can be used to compute the maximum strength under pure bending of a multiweb beam which buckles in the local mode.

## REFERENCES

1. Gerard, George: Optimum Number of Webs Required for a Multicell Box Under Bending. Jour. Aero. Sci., vol. 15, no. 1, Jan. 1948, pp. 53-56.
2. Schuette, Evan H., and McCulloch, James C.: Charts for the Minimum-Weight Design of Multiweb Wings in Bending. NACA TN 1323, 1947. ✓
3. Conway, William J.: Factors Affecting the Design of Thin Wings. Preprint No. 357, SAE Los Angeles Aero. Meeting, Oct. 5-9, 1954.
4. Semonian, Joseph W., and Anderson, Roger A.: An Analysis of the Stability and Ultimate Bending Strength of Multiweb Beams With Formed-Channel Webs. NACA TN 3232, 1954.
5. Semonian, Joseph W., and Peterson, James P.: An Analysis of the Stability and Ultimate Compressive Strength of Short Sheet-Stringer Panels With Special Reference to the Influence of Riveted Connection Between Sheet and Stringer. NACA TN 3431, 1955.
6. Anderson, Roger A., and Anderson, Melvin S.: Correlation of Crippling Strength of Plate Structures With Material Properties. NACA TN 3600, 1955.
7. Dow, Norris F., and Anderson, Roger A.: Prediction of Ultimate Strength of Skin-Stringer Panels From Load-Shortening Curves. Preprint No. 431, S.M.F. Fund Preprint, Inst. Aero. Sci., Jan. 1954.
8. Pride, Richard A., and Anderson, Melvin S.: Experimental Investigation of the Pure-Bending Strength of 75S-T6 Aluminum-Alloy Multiweb Beams With Formed-Channel Webs. NACA TN 3082, 1954.

TABLE I.- MATERIAL PROPERTIES

Property	7075-T6 (a)	2014-T6 (b)	2014-T6 (c)
E, ksi . . . .	$10.5 \times 10^3$	$10.6 \times 10^3$	$10.9 \times 10^3$
E <sub>2</sub> , ksi . . .	812	804	752
$\sigma_{cy}$ , ksi . . .	72.4	68.3	61.4
$\sigma_2$ , ksi . . .	67.8	63.3	55.6
$\epsilon_2$ . . . . .	0.00695	0.00621	0.00548

<sup>a</sup>Used in fabricated test specimens.

<sup>b</sup>Used in two-cell integral test specimens.

<sup>c</sup>Used in one-cell integral test specimens.

TABLE II.- SPECIMEN DIMENSIONS

(a) Integral beams.

Specimen	h, in.	t <sub>w</sub> , in.	t <sub>g</sub> , in.	b <sub>g</sub> , in.	c, in.	t <sub>r</sub> , in.
One-cell beams						
102-1	7.00	0.162	0.162	6.85	7.00	0.162
202	5.00	.156	.156	4.84	5.00	.156
303	4.25	.154	.154	4.09	4.25	.154
403	3.75	.153	.153	3.59	3.75	.153
502	3.50	.154	.154	3.34	3.50	.154
B-1	8.00	.115	.400	7.30	7.42	.400
B-2	8.00	.050	.400	7.25	7.30	.400
B-3	7.60	.100	.200	7.30	7.40	.200
B-4	7.60	.050	.200	7.25	7.30	.200
V-4	7.60	.050	.200	7.25	7.30	.200
Two-cell beams						
20-1	6.50	0.201	0.206	6.48	13.15	0.186
20-2	6.50	.116	.204	6.44	13.00	.187
20-3	6.50	.080	.201	6.41	12.90	.186
20-4	6.50	.062	.206	6.38	12.82	.186
32-1	6.80	.321	.328	6.50	13.32	.249
32-2	6.80	.188	.324	6.46	13.10	.248
32-3	6.80	.129	.326	6.42	12.97	.249
32-4	6.80	.102	.328	6.41	12.92	.248

TABLE II.- SPECIMEN DIMENSIONS - Concluded

(b) Fabricated beams.

Specimen	h, in.	t <sub>w</sub> , in. (a)	t <sub>g</sub> , in.	b <sub>g</sub> , in.	c, in.	t <sub>T</sub> , in.
101	3.17	0.051	0.083	1.63	5.73	0.083
102	3.15	.051	.083	2.04	6.94	.083
103	3.16	.051	.083	2.43	8.15	.083
104	3.17	.051	.082	3.22	10.58	.083
105	3.25	.051	.127	2.50	8.38	.127
106	3.25	.051	.127	3.12	10.24	.127
107	3.27	.051	.127	3.75	12.10	.127
108	3.26	.051	.126	4.98	15.84	.126
109	3.38	.051	.187	3.75	12.15	.187
110	3.38	.051	.186	4.70	14.97	.186
111	3.38	.051	.186	5.64	17.79	.186
112	3.38	.051	.183	7.54	23.45	.183
113	3.62	.051	.312	6.25	19.66	.312
114	3.62	.051	.307	7.84	24.37	.307
115	3.61	.051	.309	9.40	29.06	.309
116	3.61	.051	.310	12.54	38.46	.310

<sup>a</sup>See figure 1(d).

TABLE III.- RATIOS OF SPECIMEN DIMENSIONS

(a) Integral beams.

Specimen	$h/t_s$	$b_s/t_s$	$t_w/t_s$	$b_w/t_w$	$\beta$
One-cell beams					
102-1	43.2	42.3	1.00	42.2	1.00
202	32.0	31.0	1.00	31.0	1.00
303	27.6	26.5	1.00	26.6	1.00
403	24.5	23.5	1.00	23.5	1.00
502	22.8	21.7	1.00	21.8	1.00
B-1	20.0	18.2	.29	66.1	3.63
B-2	20.0	18.1	.12	152.0	8.40
B-3	38.0	36.5	.50	74.0	2.03
B-4	38.0	36.2	.25	148.0	4.09
V-4	38.0	36.2	.25	148.0	4.09
Two-cell beams					
20-1	31.6	31.4	0.98	31.4	1.00
20-2	31.9	31.5	.57	54.3	1.72
20-3	32.3	31.9	.40	79.0	2.48
20-4	31.6	31.0	.30	101.8	3.28
32-1	20.7	19.8	.98	20.3	.98
32-2	21.0	20.0	.58	34.7	1.74
32-3	20.8	19.7	.40	50.5	2.56
32-4	20.7	19.6	.31	63.9	3.26

TABLE III.- RATIOS OF SPECIMEN DIMENSIONS - Concluded

(b) Fabricated beams.

Specimen	$h/t_s$	$b_s/t_s$	$t_w/t_s$	$b_w/t_w$ (a)	$\beta$
101	38.2	19.6	0.6	59	3.0
102	38.0	24.6	.6	59	2.4
103	38.1	29.3	.6	59	2.0
104	38.6	39.3	.6	59	1.5
105	25.6	19.7	.4	59	3.0
106	25.6	24.6	.4	59	2.4
107	25.8	29.5	.4	59	2.0
108	25.9	39.6	.4	59	1.5
109	18.1	20.0	.3	59	3.0
110	18.1	25.2	.3	59	2.3
111	18.2	30.3	.3	59	2.0
112	18.5	41.1	.3	59	1.4
113	11.3	20.0	.2	59	3.0
114	11.8	25.5	.2	59	2.3
115	11.7	30.4	.2	59	2.0
116	11.7	40.5	.2	59	1.5

<sup>a</sup>See figure 1(d).

TABLE IV.- MAXIMUM BENDING MOMENTS

(a) Integral beams.

Specimen	$\sigma_s$ , ksi	Computed skin moment, in-kips, (a)	Experimental failing moment, in-kips	$M_w$ per web, in-kips	$\frac{M'_i}{b_w^2}$ , ksi	$\frac{M'_i}{\sigma_2 b_w^2}$
One-cell beams						
102-1	31.0	236	444	104	0.323	0.00510
202	42.5	155	<sup>b</sup> 263	54	.473	.00748
303	49.6	127	<sup>b</sup> 201	37	.542	.00862
403	56.0	111	<sup>b</sup> 159	24	.508	.00803
502	60.6	104	<sup>b</sup> 142	19	.510	.00808
B-1	62.3	1,380	1,560	90	.213	.00337
B-2	62.5	1,380	1,385	(c)	(c)	(c)
B-3	36.0	390	510	60	.150	.00237
B-4	36.3	390	446	(c)	(c)	(c)
Two-cell beams						
20-1	44.6	750	1,075	108	0.420	0.00664
20-2	44.4	734	850	39	.153	.00242
20-3	44.0	716	730	5	.018	.00029
20-4	45.3	740	720	(c)	(c)	(c)
32-1	68.0	1,890	2,450	187	.678	.01071
32-2	67.8	1,850	2,100	83	.302	.00477
32-3	68.4	1,860	1,980	40	.147	.00232
32-4	68.5	1,880	1,940	(c)	(c)	(c)

<sup>a</sup>Computed skin moment for one-cell beams equals  $M_s$ ; computed skin moment for two-cell beams equals  $2M_s$ .

<sup>b</sup>Average of two tests.

<sup>c</sup>Values not calculated because specimens did not satisfy minimum web-thickness requirements of equations (9).

TABLE IV.- MAXIMUM BENDING MOMENTS - Concluded

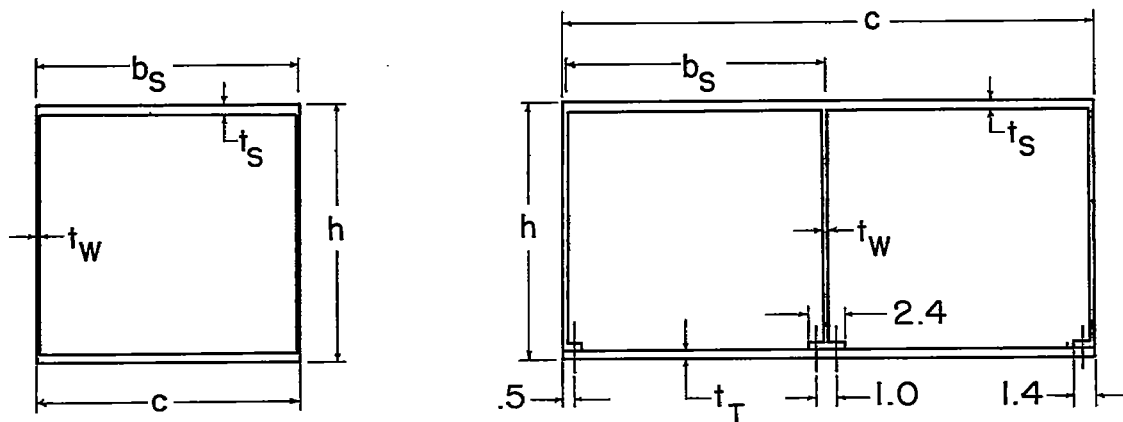
(b) Fabricated beams.

Specimen	$\sigma_s$ , ksi	Computed skin moment, in-kips (a)	$4M_w$ , in-kips	$4M_a$ , in-kips	Total computed failing moment, in-kips	Experimental failing moment, in-kips
101	69.9	102	30	38	170	165
102	57.7	104	30	38	172	164
103	48.4	105	30	38	173	163
104	36.0	104	30	38	172	161
105	69.9	231	30	38	299	<sup>b</sup> 285
106	57.7	238	30	38	306	307
107	48.0	238	30	38	306	293
108	35.9	236	30	38	304	308
109	69.5	503	30	38	571	562
110	56.1	504	30	38	572	576
111	46.8	505	30	38	573	540
112	34.4	487	30	38	555	561
113	<sup>c</sup> 48.5	<sup>c</sup> 985	30	40	1,055	1,070
114	<sup>c</sup> 39.3	<sup>c</sup> 973	30	40	1,043	1,020
115	46.6	1,400	30	40	1,470	1,370
116	35.0	1,405	30	40	1,475	1,355

<sup>a</sup>Computed skin moment for three-cell fabricated beam equals

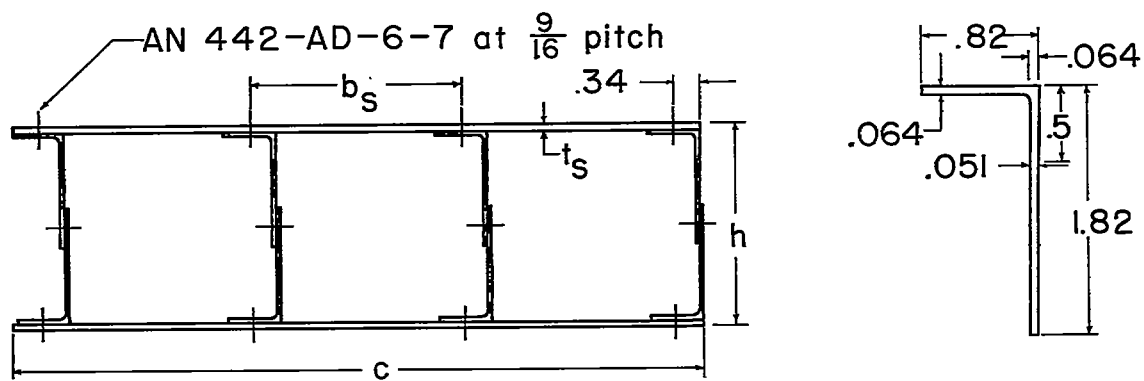
$3\sigma_s b_s t_s b_w + \sigma_2 (c - 3b_s) t_s b_w$ . The second term is the moment carried by the skin overhanging the exterior webs. (See fig. 1(c).)

<sup>b</sup>Average of two tests.<sup>c</sup>Calculated from web-crushing considerations; computed skin moment for this condition equals  $\sigma_s c t_s b_w$ .



(a) One-cell integral beam.

(b) Two-cell integral beam.



(c) Three-cell fabricated beam.

(d) Angle extrusion.

Figure 1.- Test specimens. All dimensions are in inches.

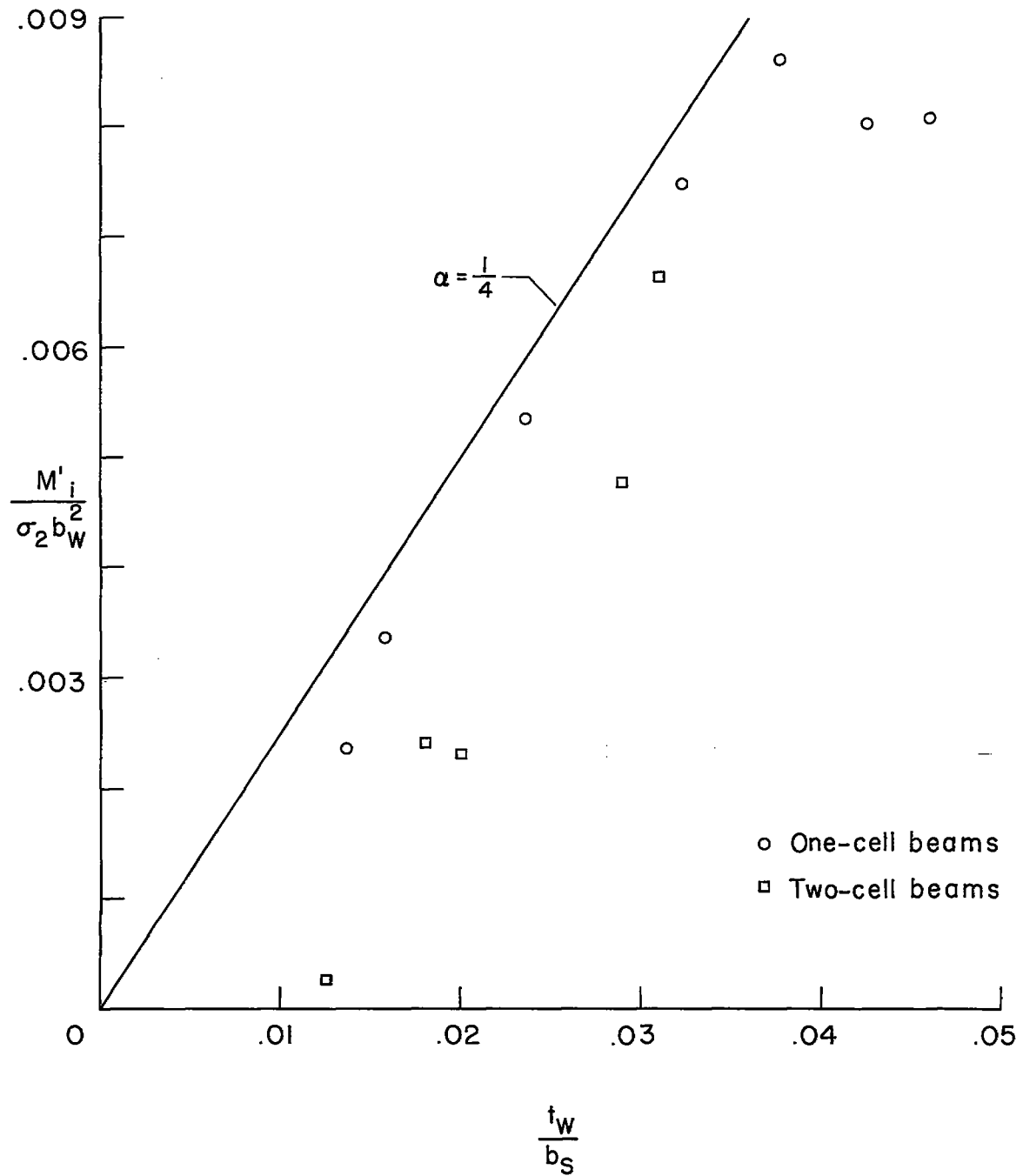


Figure 2.- Maximum bending moment resisted by webs of integral test specimens.

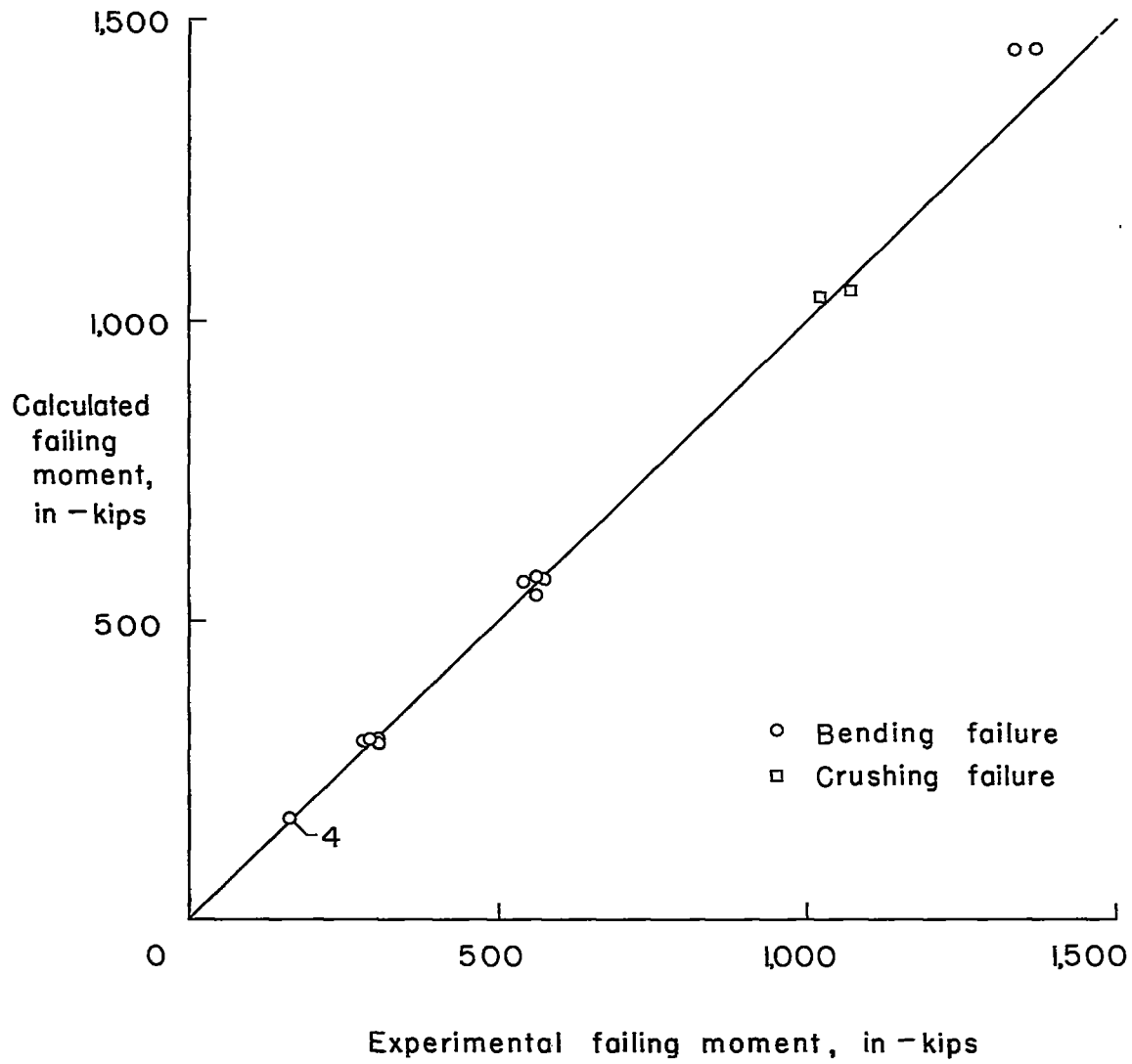


Figure 3.- Comparison of calculated and experimental failing moments for fabricated test specimens.

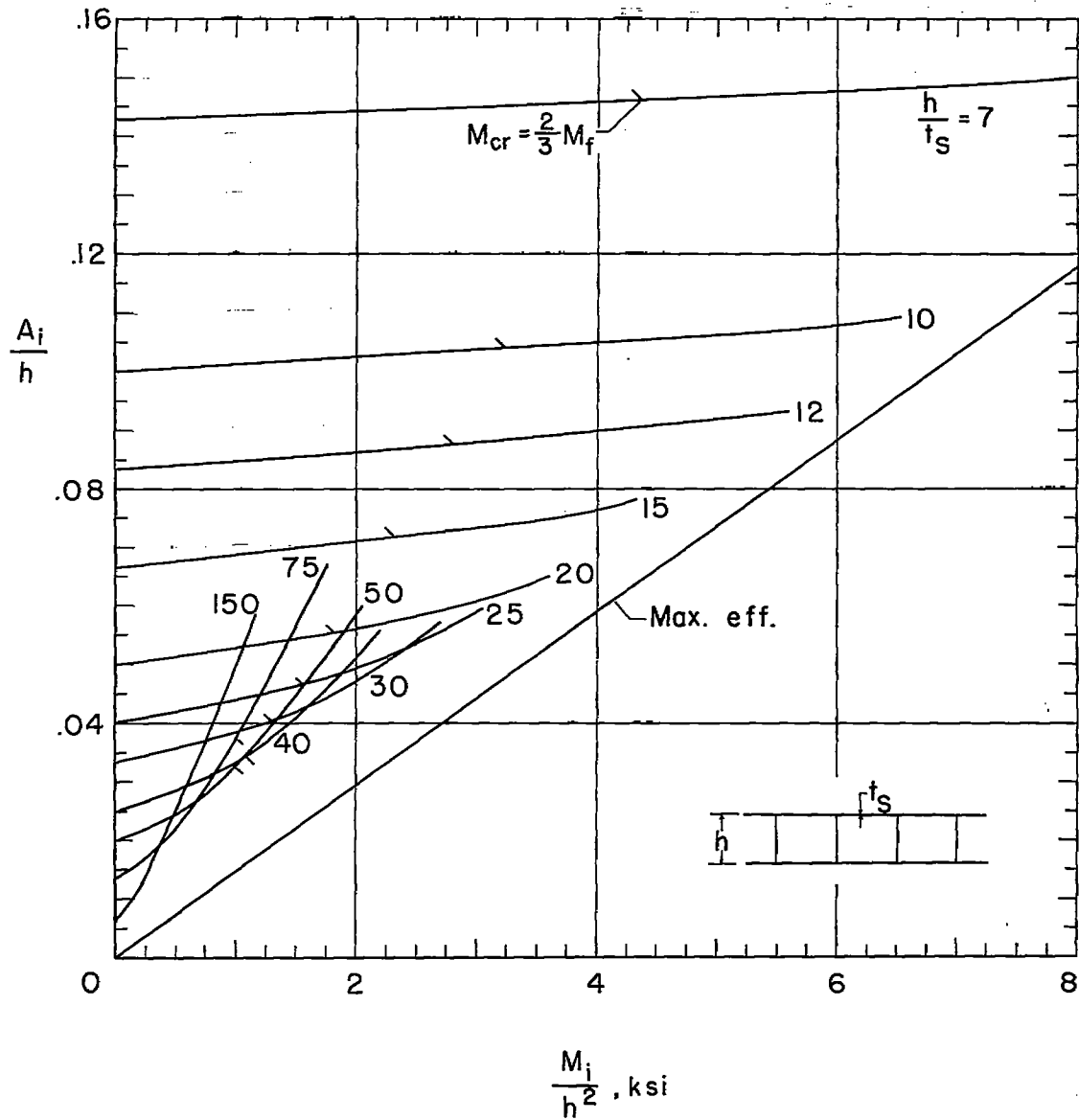


Figure 4.- Multiweb-wing efficiency chart for 7075-T6 aluminum-alloy structures. Tick marks on curves indicate buckling at limit load.

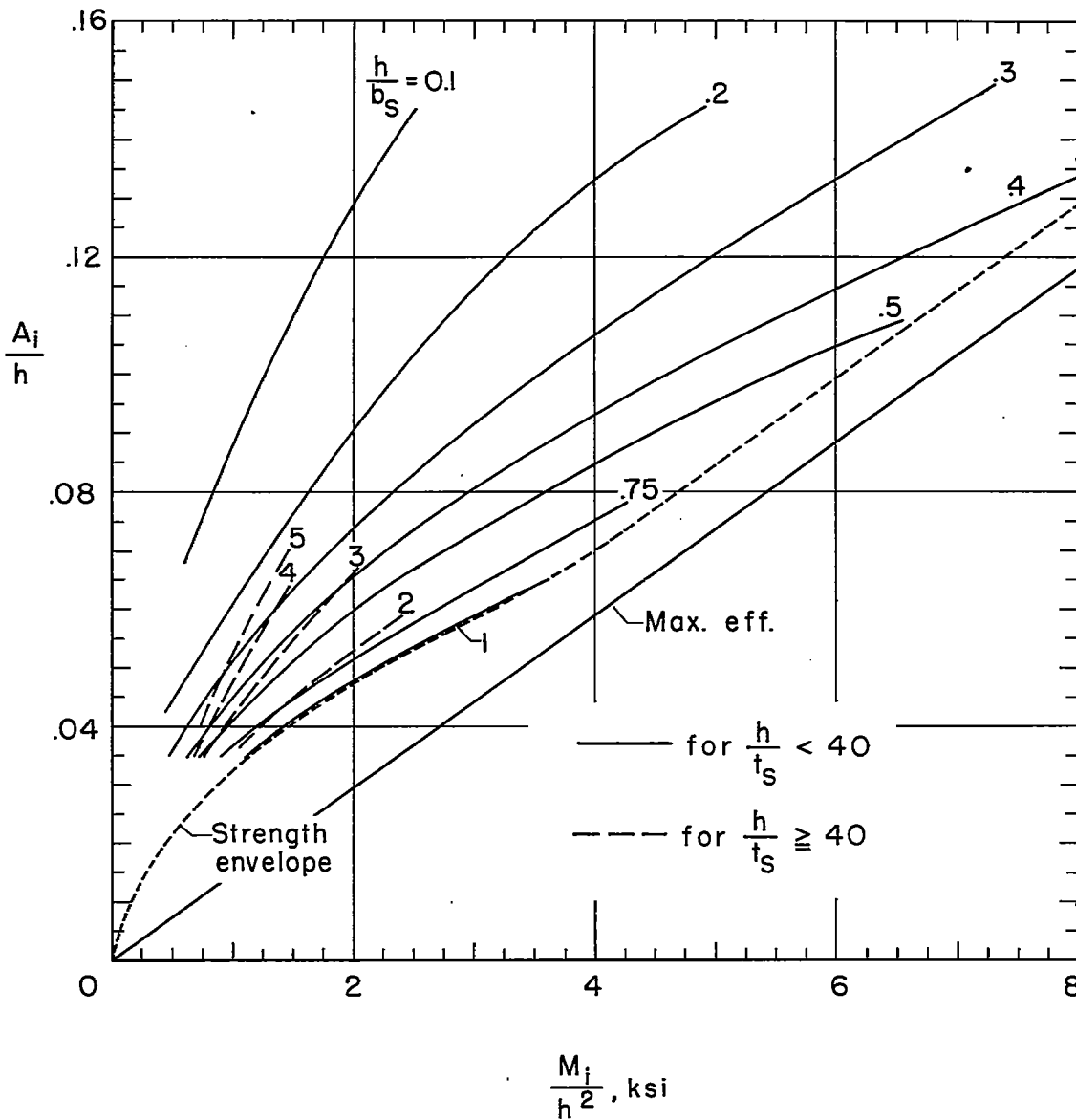


Figure 5.- Alternate form of multiweb-wing efficiency chart for 7075-T6 aluminum-alloy structures.

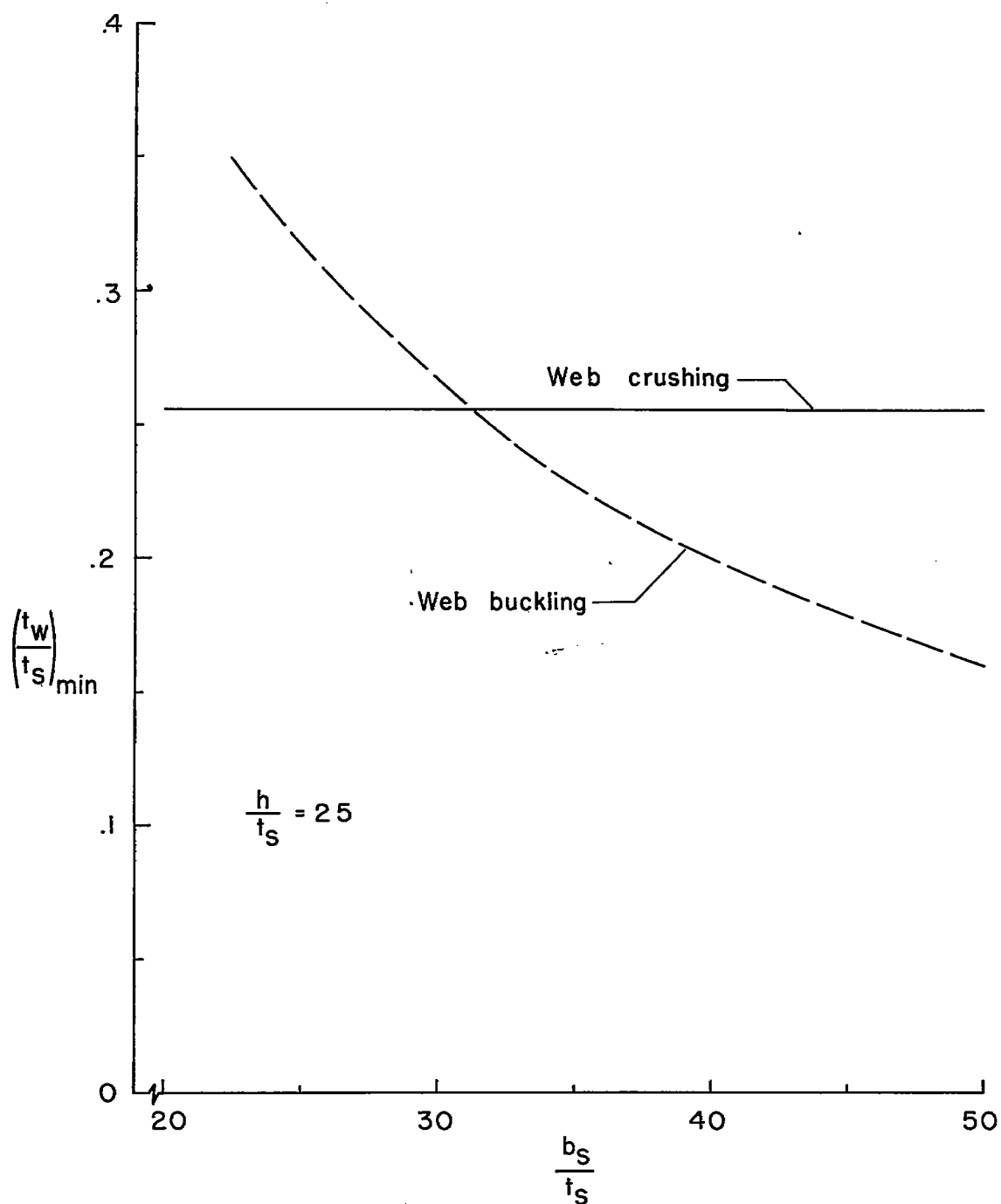


Figure 6.- Typical curves of minimum web-thickness requirements.